Coordination of microtubule and microfilament dynamics by *Drosophila* Rho1, Spire, and Cappuccino

Alicia E. Rosales-Nieves[1,2], James E. Johndrow[1,2], Lani C. Keller[1,2], Craig R. Magie[1], Delia M. Pinto-Santini[1] and Susan M. Parkhurst[1,3]

[1]Division of Basic Sciences, Fred Hutchinson Cancer Research Center, 1100 Fairview Avenue North, Seattle, Washington 98109-1024, USA

[2]These authors contributed equally to this work.

[3]Correspondence should be addressed to S.M.P (email: susanp@fhcrc.org)

The actin nucleation factors Spire and Cappuccino regulate the onset of ooplasmic streaming in *Drosophila*[1-5]. Although this streaming event is microtubule-based, actin assembly is required for its timing. It is not understood how the interaction of microtubules and microfilaments is mediated in this context. Here we demonstrate that Cappuccino and Spire have microtubule and microfilament crosslinking activity. The *spire* locus encodes several distinct protein isoforms (SpireA, SpireC, and SpireD). SpireD was recently shown to nucleate actin, but the activity of the other isoforms has not been addressed. We find that SpireD does not have crosslinking activity, while SpireC is a potent crosslinker. We show that SpireD binds to Cappuccino and inhibits F-actin/microtubule crosslinking, and activated Rho1 abolishes this inhibition, establishing a mechanistic basis for the regulation of Capu and Spire activity. We propose that *Rho1*, *cappuccino* and *spire* are elements of a conserved developmental cassette that is capable of directly mediating crosstalk between microtubules and microfilaments.

Cytoskeletal elements must be coordinately regulated for cells to carry out complex functions, such as the cytoplasmic movements required to disperse or localize intracellular components[5]. The formin homology (FH) protein Cappuccino (Capu) and the WASP homology 2 (WH2) domain-containing protein Spire are both required for the proper timing of one such cytoplasmic movement, ooplasmic streaming in *Drosophila*[1,3]. In wildtype oocytes, vigorous ooplasmic streaming is associated with rapid growth during stages 10b-13, and is never observed prior to this stage. Mutations in *capu* and *spire* result in premature ooplasmic streaming, beginning at stage 7/8 and continuing through stage 13. This premature streaming interferes with transport mechanisms required for the localization of early polarity markers, resulting in disruption of dorsal-ventral and anterior-posterior body axes[1,2]. Both the wildtype streaming event and the premature streaming in *capu* and *spire* mutants are microtubule-based[1]. Streaming never takes place in oocytes lacking kinesin, and colcemid injection blocks premature streaming in these mutants[5,6]. Recent work suggests that streaming is restrained by the competing effects of dynein and kinesin, and can be initiated by blocking dynein function[7]. Thus, it is somewhat paradoxical that Spire and Capu nucleate actin, but are not known to affect microtubule architecture or dynamics. Interestingly, the premature streaming seen in *capu* and *spire* mutant oocytes can be recapitulated by injection of the actin-depolymerizing drug cytochalasin D into wildtype oocytes, suggesting that actin assembly may restrict microtubule rearrangements required for ooplasmic streaming[8]. Presumably, microtubule and microfilament dynamics are coordinated in oogenesis by a group of proteins that includes Spire and Capu, as well as one or more upstream signals. However, the signaling events that combine to encode a "switch" from the non-streaming to streaming mode of the oocyte cytoskeleton, and how these signals are translated to coordinate changes in microtubule/microfilament dynamics and architecture are not known.

We previously showed that double heterozygosity for loss-of-function alleles of the small GTPase *Rho1* and *capu* results in 100% maternal effect lethality and abnormal microfilament architecture at the oocyte cortex[9]. Here we refer to these doubly heterozygous females as "*Rho1-capu*" (see Supplementary Information, Fig. S1). To determine if maternal lethality in *Rho1-capu* is due to premature ooplasmic streaming, we visualized cytoplasmic movements in *Rho1-capu* oocytes by timelapse confocal imaging of yolk granule fluorescence. Like *capu* mutants, these oocytes exhibit premature ooplasmic streaming beginning at stage 8 of oogenesis (Fig. 1c-

c' and Supplementary Movie 1c). Similarly staged *Rho1-capu* oocytes assemble prominent subcortical arrays of microtubules consistent with ooplasmic streaming (Fig. 1h; and see Supplementary Information, Fig. S2). We next asked whether the Rho1 mutation results in the same phenotype. Germlines genetically lacking Rho1 do not progress far enough to assess the role of Rho1 in ooplasmic streaming[9]. Thus, we have used two approaches to modulate the level of Rho1 activity during oogenesis. The *wimp* mutation, which reduces transcription at the *Rho1* locus, was used in *trans* to loss-of-function alleles of Rho1, mimicking a hypomorphic mutation (designated *reduced Rho1*)[9]. We also injected C3 transferase[10], a specific peptide inhibitor of Rho, directly into wildtype oocytes. Reduced *Rho1* and C3-injected oocytes both exhibit premature ooplasmic streaming, and subcortical arrays of microtubules are observed in reduced *Rho1* at stage 8 (Fig. 1d-d', i; see Supplementary Information, Fig. S3a; and see Supplementary Movies 1d and 1f; see Methods). Interestingly, we find that *spire* and *capu* also exhibit a dominant genetic interaction (100% maternal-effect lethal). Doubly heterozygous *capu*/*spire* mutants stream prematurely and have a similar microtubule phenotype to *Rho1 capu* and reduced *Rho1* (Fig. 1e-e', j, and see Supplementary Movie 1e; see Methods). This is consistent with the hypothesis that these proteins are both required to regulate the same molecular events *in vivo*[11].

Although *capu* and *spire* have identical mutant phenotypes, the localization of these proteins has not been addressed during oogenesis, the only developmental stage at which they are essential[2]. We made GFP-fusion constructs of *capu* as well as *spire* (isoforms D and C; see Fig, 3b) and expressed them in the germline using the UAS-Gal4 system[12]. We find that Capu and SpireD (a WH2-domain containing Spire isoform) are enriched at the cortex of both nurse cells and oocyte, and are diffusely distributed throughout the cytoplasm of these cells (Fig. 2a-b' and see Supplementary Information, Fig. S3b-c'). Both are found at much higher levels in the nurse cells than in the oocyte, and do not exhibit asymmetry. In contrast, SpireC-GFP is found in punctate structures throughout the germline, and also associates with the oocyte cortex (Fig. 2c-c' and see Supplementary Information, Fig. S3d-d'). Notably, a Rho1-GFP construct under endogenous control mirrors the higher cortical accumulation of Capu and Spire C/D (Fig. 2d-d' and see Supplementary Information, Fig. S3e-e').

In mammalian cells, Rho acts through Diaphanous-related formins (DRFs), the microtubule plus-end binding (+TIP) protein Eb1, and Adenomatous Polyposis Coli (APC), to stabilize microtubules[13-15]. We investigated the possibility that microtubule stability may be important in

the regulation of ooplasmic streaming by staining oocytes with an antibody specific to the detyrosinated form of α-tubulin (Glu-α-tubulin) that outlines stable microtubules. In wildtype oocytes, Glu-microtubules are restricted to the cortex, and are relatively less abundant at the posterior pole, mirroring the overall distribution of oocyte microtubules (Fig. 2g, h-h''). In *Rho1-capu* and reduced *Rho1* oocytes, Glu-microtubules remain restricted to the cortex, but no reduction in Glu-tubulin is visible at the posterior pole relative to the rest of the cortex (Fig. 2g, i-j''). This likely reflects the overall loss of oocyte microtubule polarity that is observed in *capu* and *spire* mutants (see Supplementary Information, Fig. S1)[1-4]. Thus, it appears that the mechanism through which Rho1 controls microtubule dynamics in *Drosophila* oogenesis is distinct from that in mammalian cells. Importantly, we find that Capu, Rho1, and Spire show higher accumulation in the only region of the oocyte where microtubules are closely juxtaposed to microfilaments (see Fig. 2e, f), raising the possibility that these proteins participate directly in microtubule/microfilament crosstalk.

Although DRFs are well-characterized Rho effectors[16-18], it has not yet been established if Rho regulates the activity of non-DRF formins. However, our genetic data implicate Rho1 in regulating the timing of ooplasmic streaming, so we asked whether this phenotype reflects a direct interaction between Rho1 and Spire or Capu. We find that SpireD, SpireC, and Capu bind to Rho1 in GST-pulldown assays showing a preference for Rho in its GTP-exchanged active state (Fig. 3c,d; see Supplementary Information, Fig. S4). We mapped the binding sites for Rho1 on SpireD, SpireC, and Capu to specific regions using smaller protein constructs in pulldown assays (Fig. 3e,f). Rho1 binds to the WH2-domain containing region of SpireD3 (Fig. 3b, e) and to SpireC3 (Fig. 3b, f), which contains the conserved Spire-box and FYVE domains, as well as the JNK-binding site. The Rho1-binding region of Capu (CapuN3; aa 125-250) is N-terminal to the FH1-FH2 module and does not contain any previously characterized domains (Fig. 3a,c). We have designated this domain as the Rho-binding domain (RhBD*). We also immunoprecipitated Capu from ovary lysate with a Rho1-monoclonal antibody[19], confirming the *in vivo* relevance of this interaction (Fig. 3g; antibodies to Spire are not yet available).

DRF proteins are thought to be regulated through an inhibitory intra-molecular interaction between the conserved N-terminal Rho binding and C-terminal Diaphanous autoinhibitory (DAD) domains that is relieved by Rho GTPase binding[16,18,20-23]. Although Capu does not have a DAD domain, because of its interaction with Rho1 we thought it possible that Capu activity is

regulated by an autoinhibitory mechanism. Although CapuN and CapuC associate *in vitro* (Fig. 3h), we do not observe any autoinhibitory effect of CapuN on actin nucleation by CapuFH2 (Fig. 4b) or in actin/microtubule crosslinking assays (Fig. 5d) suggesting that this self-association may not have biological relevance in the context of oocyte development. We next considered the possibility that Spire might play a role in the regulation of actin nucleation by Capu. In support of this hypothesis, the two loci interact genetically, and the FH2 domain of Capu binds to SpireD *in vitro* (Fig. 3i). We mapped this interaction to a smaller construct, SpireD3, which contains the four tandem WH2-domains and the Rho1 binding site (Fig. 3i). We then conducted actin polymerization assays to determine whether this interaction is inhibitory. However, we did not observe any inhibition of actin nucleation activity when either CapuFH1-FH2 (CapuC1) or CapuFH2 were pre-incubated with various concentrations (ranging from equimolar to 5-fold excess Spire construct) of SpireD or SpireD3 (Fig. 4f and data not shown).

To address the question of whether actin nucleation is sufficient to prevent premature onset of ooplasmic streaming, we took advantage of the fact that several alleles of *capu* that have been shown to cause premature streaming have mutations in the FH2-domain[8]. We expressed and purified CapuFH2 constructs with the point mutations L768H and P597T, corresponding to the strong allele $capu^{RK12}$ and weak allele $capu^{2F}$, respectively. The L768H mutation results in complete loss of nucleation activity *in vitro* (Fig. 4c), yet CapuFH2(L768H) is still able to dimerize (Fig. 3k), suggesting that this mutation creates a nucleation-dead FH2 domain. Interestingly, the P597T mutation does not substantially affect the nucleation activity of CapuFH2 (Fig. 4c), suggesting that nucleation is not solely responsible for the premature streaming phenotype.

Since both $capu^{RK12}$ and $capu^{2F}$ mutants stream prematurely, we asked whether the mutation corresponding to the $capu^{2F}$ lesion disrupts some other essential function of the Capu protein. Based on the localization of Rho1, Capu, and Spire at the oocyte cortex and apparent coordination of microtubules and microfilaments required to regulate the onset of ooplasmic streaming, we hypothesized that rather than regulating only actin dynamics and affecting microtubule dynamics indirectly, these proteins are involved directly in this coordination. To address this possibility, we performed *in vitro* microtubule/microfilament crosslinking assays[24] using purified recombinant proteins. Interestingly, CapuN1 demonstrated a potent actin filament bundling activity (Fig. 5b), whereas CapuFH2 crosslinks F-actin and microtubules (Fig. 5c).

Consistent with this result, we find that CapuN1 binds to F-actin while CapuFH2 binds to both F-actin and microtubules in co-sedimentation assays (see Supplementary Information, Fig. S5a). Moreover, CapuN1 exhibits self-association in pulldown assays (data not shown), suggesting that it bundles F-actin through dimer- or oligomerization and likely has a single actin-binding domain. The minimum Capu construct with bundling activity (aa250-415) establishes a new F-actin binding domain in a region of the protein that is not homologous to other known actin-binding proteins. We also tested the crosslinking activity of CapuFH2[L768H] and CapuFH2[P597T], and found that the L768H mutation, which results in a more penetrant phenotype *in vivo*, also abrogates crosslinking activity (Fig. 5f, and see Supplementary Information, Fig. S5b). However, the CapuFH2[P597T] construct shows attenuated crosslinking activity (Fig. 5e, and see Supplementary Information, Fig. S5b), indicating that the phenotype observed in *capu*^{2F} mutants may be due at least in part to loss of this function. This also suggests that Capu-mediated actin nucleation is not sufficient to prevent premature ooplasmic streaming.

We also investigated whether SpireD and SpireC have any crosslinking/bundling activity. We find that SpireC, which lacks the four tandem WH2-domains that are sufficient for actin nucleation *in vitro*, has bundling and crosslinking activity similar to that of CapuFH2 (Fig. 5g). However, the actin nucleating isoform SpireD has no crosslinking or bundling activity (Fig. 5h). In light of the distinct subcellular distribution of SpireD and SpireC (see Fig. 2b-c', and see Supplementary Information. Fig. S3c-d'), this data suggests that the C and D isoforms of Spire regulate distinct aspects of cytoskeletal architecture.

We next asked whether the crosslinking activity of CapuFH2 is affected by the presence of Spire. When added at equimolar ratios with Capu, SpireD and SpireD3 entirely block crosslinking and microtubule bundling (Fig. 5i, k), whereas SpireD1, SpireD2 and SpireD4 have no affect (Fig. 5j; data not shown). Notably, we find that addition of equimolar activated Rho1 (Rho1-GDP-pNPP), but not inactive Rho1 (Rho1-GDP), restores crosslinking and microtubule bundling by CapuFH2 in the presence of SpireD (Fig. 5l, m, respectively), and can compete with the binding of SpireD to CapuFH2 in pulldown assays (Fig. 3j). As the microtubule bundling and crosslinking activities of SpireC are similar to that exhibited by CapuFH2, we examined the affect of SpireD on SpireC bundling and crosslinking. SpireD similarly blocks crosslinking by SpireC, but did not affect its ability to bundle microtubules (Fig. 5n). In contrast to the interaction between CapuFH2 and SpireD, addition of activated Rho1 does not restore

crosslinking by SpireC in the presence of SpireD (data not shown). These new bundling and crosslinking activities raise the possibility that Capu and Spire regulate the onset of ooplasmic streaming by directly mediating coordination of actin assembly and microtubule architecture. Moreover, our finding that Rho1 relieves the inhibition of CapuFH2-mediated crosslinking by SpireD provides a mechanistic basis for the genetic interaction of *Rho1*, *capu*, and *spire*.

Our results suggest that Rho1 regulates the timing of ooplasmic streaming by regulating the microtubule/microfilament crosslinking that occurs at the oocyte cortex. In this model, crosslinking antagonizes the formation of the dynamic subcortical microtubule arrays that are required for ooplasmic streaming (Fig. 5o-p). We propose that activated Rho1 transduces a signal during stages 8-10b that promotes the crosslinking activity of Capu and SpireC by preventing binding of SpireD to both Capu and SpireC (Fig. 5o). Rho1 then becomes inactivated at stage10b, presumably by a signaling event, allowing SpireD to bind to Capu and SpireC, thereby inhibiting microtubule/microfilament crosslinking (Fig. 5p). When signaling through this pathway or the level of Capu and/or Spire protein is reduced through mutation, ooplasmic streaming occurs constitutively from stage 8 through 13, resulting in the severe patterning defects observed in these mutants (see Supplementary Information, Fig. S6). That SpireD also inhibits the crosslinking activity of SpireC suggests that a parallel regulatory mechanism exists for SpireC mediated crosslinking. Although we cannot rule out a role for Rho1 in regulating actin nucleation by Capu and Spire, the mechanism established here by which Spire and Rho1 regulate the crosslinking activity of Capu does not seem pertinent to actin nucleation. Viewed in light of the fact that the P597T mutation in the FH2 domain, which is encoded by the *capu*^{2F} allele, does not affect actin nucleation activity but is less efficient at crosslinking microtubules and microfilaments, the crosslinking activity we describe appears to be an important aspect of how ooplasmic streaming is regulated *in vivo*.

The data presented herein have several broader implications. The finding that Capu and Spire regulate each other's activity suggests an explanation for the conserved co-expression of these two *de novo* actin nucleation factors[25], both of which create linear actin filaments[11,16,18] and are required to mediate the same developmental events[2]. Moreover, this work establishes Rho1 as a direct regulator of a broader group of actin nucleating proteins, and is the first evidence for how the activity of Spire and Capu is regulated to coordinate the ooplasmic streaming event *in vivo*. The direct interaction between Rho1 and Capu suggests an additional level of complexity

to this mechanism. It is thus possible that Rho1 may simultaneously regulate the nucleation and crosslinking activities of Capu through an as yet unclear mechanism, further investigation of which will require the expression of full-length Cappuccino constructs that contain the relevant binding site.

To date, much work has been devoted to understanding the role of formins, and more recently Spire, in controlling actin dynamics and nucleation. However, DRF proteins also have profound affects on microtubule dynamics and stability, with recent evidence indicating that these affects are at least in some cases independent of the actin nucleation function[14,15]. The data presented here suggest that direct regulation of microtubule architecture may be a property common to a larger subset of formins, as well as to at least one of the Spire protein isoforms. The distinct mechanism by which Spire and Capu regulate microtubule/microfilament crosstalk is consistent with the highly specialized function of these proteins in regulating germline development in *Drosophila*. Indeed, the mammalian homologue of *capu*, *formin-2*, is also required only in the female germline, where it regulates proper chromosome segregation, another process involving intimate coordination of microtubule and microfilament dynamics[26]. Recently, mutation at the formin-2 locus has been implicated in unexplained female infertility in humans[27]. Thus, *capu* and *spire* appear to be elements of a highly conserved cassette that is required for the very earliest stages of metazoan development. Precisely how the activity of these proteins is coordinated with developmental signaling circuits to allow for the proper regulation of ooplasmic streaming or chromosome segregation will certainly provide interesting venues for future work.

METHODS

Fly Strains and Genetics. Flies were cultured and crossed on yeast-cornmeal-molasses-malt and maintained at 25ºC in 50% humidity. The alleles used in this study were *capu*^{RK12}, *capu*^{EY12344}, *Rho1*^{1B}, and *spire*^{2F}. All of these alleles were described previously with the exception of *capu*^{EY12344}, which contains a P-element insertion in the first common exon of the *capu* ORF and is a putative null allele. The *wimp* mutation was described previously[19]. GFP-Rho1 transgenic flies contain a GFP-*Rho1* fusion gene that is expressed under the control of the endogenous *Rho1* promoter. A ~7 kb *Hind*III-*Mlu*I genomic fragment encompassing the entire *Rho1* gene was subcloned into the Casper transformation vector, and intronic regions were removed by substituting cDNA sequence for genomic between the ATG and stop codons. GFP was fused in frame at the ATG of *Rho1*. GFP expression in transgenic flies carrying this RhoGFP fusion is indistinguishable from Rho1 expression detected by antibody staining (data not shown), except in the rare cases (~10%) where the transgene exhibits mosaicism in the somatic (follicle) cells. Images of such mosaic egg chambers are included in this manuscript in order to more easily visualize the localization of Rho1 relative to the oocyte cortex. GFP-Capu was created by fusing GFP upstream of the ATG of CapuRA. This GFP-Capu fusion construct was cloned into pUASp as a *Kpn*I-*Bam*HI fragment and used to make germline transformants as described[28]. GFP-SpireC and GFP-SpireD were made as described above for Capu, except that the fusions were made to the ORFs of SpireRC or SpireRD, respectively. UAS transgenes were expressed in the germline using pCog:Gal4; NGT40:Gal4; VP16nos:Gal4 triple maternal driver lines[29]. All transformant lines used in this study were mapped to a single chromosome and shown to have non-lethal insertions.

Immunofluorescence. Female flies were fattened for two days on yeast-cornmeal-molasses-malt with supplemental dried active baker's yeast at 25°C. Ovaries were dissected into *Drosophila* Ringer's buffer at room temperature and fixed using 1xPBS/6% formaldehyde/heptane. After three washes with PTW (1xPBS/0.1% tween-20), ovaries were permeablized in 1% triton X-100 for 2 hours at room temperature and blocked using PAT (1xPBS/0.1%tween-20/1% BSA/0.05% Azide) for two hours at 4 degrees (the subsequent steps are performed at 4 degrees). Antibodies were added at various concentrations (see below) in PAT, and ovaries incubated overnight (approximately 24 hours) with primary antibody. Primary antibody was then removed and ovaries washed 3 times with GNS (1xPBS/0/1% tween-20/0.1% BSA/2% normal goat serum) for 30 minutes each. Secondary antibody (Alexa conjugates, Invitrogen) in PbT (1xPBS/0.1% tween/0.1% BSA/0.05% Azide) was then added as appropriate (1:500-1:4000), and incubated over two nights (approximately 36 hours). Ovaries were washed 6-8 times with PTW, and mounted in 1xPBS/70% glycerol, flattened slightly, and visualized by confocal microscopy. For microtubule visualization, ovaries were dissected into room temperature Robb's medium (55mM KOAc, 40mM NaOAc, 100mM sucrose, 10mM glucose, 1.2mM $MgCl_2$, 1.0mM $CaCl_2$, 100mM HEPES, pH 7.4) for a maximum of eight minutes, and were fixed and stained immediately thereafter as previously described[30], using FITC-labeled anti-α-tubulin monoclonal antibody DM1A (Sigma), or clone 1D5 anti-Glu-α-tubulin (1:250; Synaptic Systems) directly labeled using either an AlexaFluor monoclonal antibody labeling kit (Invitrogen) or a Zenon labeling kit (Invitrogen) and used at 1:200. Immunofluorescence of embryos was performed as described[12]. The following antibodies were used in this study: α-vasa (1:250, P. Lasko), α-oskar (1:3000, A. Ephrussi), α-phosphotyrosine (1:1000, clone 4G10,

Upstate), α-staufen (1:1000, D. St. Johnston). DAPI was used at 1μg/mL and AlexaFluor-labeled phalloidin (Invitrogen) at 3 units/assay.

Confocal Microscopy. Visualization was by confocal microscopy using a Zeiss LSM 510 META with excitation at 488nm or 543nm and collecting emission using a BP-505-550, BP-560-615, or LP-560 filter. In some cases, a Leica Confocal microscope with 488nm and 568nm laser lines was used. For DAPI we used a two-photon 780nm laser line and BP415-450 filter. We used a Plan-Neofluor 40x/1.3 Oil or Plan-Apochromat 20x/0.75 dry objective for imaging these samples.

Live Imaging. For live imaging, females were fattened as above and injected in the abdomen with 0.4% trypan blue in normal saline. Two hours after injection, ovaries were dissected into ovarioles in halocarbon 700 oil on glass-bottom culture dishes (bioptechs). As noted for other premature streaming mutants[7,30], we have observed some variation with respect to the speed of ooplasmic streaming in wildtype and for the mutants described herein (and even in the later stages for wildtype). We find that *Rho1-wimp* mutants always exhibit slower streaming, most likely due to the inability to completely eliminate Rho1 from the germline. For injection of C3 transferase, wildtype egg chambers were dissected into halocarbon series 700 oil then injected with GST-C3 transferase in injection buffer (5mM KCl, 0.1mM Na_2PO_4 pH 6.8) using a microinjection apparatus. Concentrations of 10-50nM resulted in premature ooplasmic streaming, whereas higher concentrations (100nM and above) resulted in rapid yolk granule aggregation at the oocyte cortex (data not shown). Time-lapse movies were recorded by taking images of a single 1-2 micron central section of the oocyte every 10 seconds on a Zeiss LSM 510 META confocal microscope. Excitation used a 543nm laser and detection used a 560 long pass filter. Projected images represent six consecutive time points. All movies are provided at 30x real time.

Plasmids and Constructs. This study used the following constructs: CapuN (amino acids 1-415), CapuN2 (amino acids 1-250) CapuN3 (amino acids 125-250), CapuC1 (amino acids 415-1058), CapuC2 (amino acids 900-1058), CapuFH1-FH2 (amino acids 462-1058), CapuFH2 (amino acids 584-1058), SpireD (amino acids 1-488 of SpirePD) SpireD3 (amino acids 366-491 of SpirePD), Spire D1 (amino acids 1-198 of SpirePD), SpireC (full-length SpirePC), SpireC3 (amino acids 190-626 of SpirePC) Rho1 (full-length Rho1-PA), DN-Rho1(T19N), and CA-Rho1(G14V). These constructs were cloned into pCite (Novagen), pGEX (GE), or pRSET (Stratagene) vectors using standard PCR cloning techniques.

Protein Expression. Constructs in pGEX or pRSET vectors were transformed into Rosetta-Gami B BL21(DE3) pLysS strains (Novagen). Cultures were inoculated and grown overnight at 37°C, diluted tenfold, and grown to OD_{600}=0.8-1.0. Expression was induced with 50μM IPTG, cultures were transferred to 18°C, and grown overnight (at least 18 hours). Cells were lysed by sonication, freeze-thaw, and endogenous lysozyme expression from pLysS in lysis buffer (50mM Tris pH 7.6, 100-300mM NaCl, 5% glycerol, 5mM DTT) with Complete protease inhibitor tablets (Roche) or Phenylmethylsulfonyl fluoride (PMSF). Triton X-100 was added to 1% and lysates were incubated at 4°C for 30 minutes, and sonicated further as required. Lysates were centrifuged at 10,000 rpm for 30 minutes in a JA-17 or SS-34 rotor and the supernatants were coupled to Glutathione-sepharose 4B (GE) or Fastflow Nickel-Sepharose 6 (GE) by 1-2 hour

incubation at 4°C. The matrix was washed three times with lysis buffer (without protease inhibitors, and including 10mM Imidazole in the case of HIS-tagged constructs) and eluted two times one hour with elution buffer (50mM Tris pH 8.0, 150mM NaCl, 5% glycerol, 5mM DTT, 20mM reduced glutathione or 200mM Imidazole). Elutions were pooled, concentrated as necessary using centricon/centriprep/microcon centrifugal filter devices (Millipore), dialyzed into G-Buffer -ATP (2mM Tris pH 8.0, 0.1mM $CaCl_2$) +5% glycerol, flash frozen in G-Buffer (as above +0.1mM ATP) +50% glycerol, and stored at –80ºC. In the case of C3 transferase, we dialyzed the elutions into injection buffer (5mM Kcl, 0.1mM $NaPO_4$ pH 6.8), and stored at 4ºC. For GST-pulldown assays, proteins were expressed and purified as above, except that HEPES was used instead of Tris. GST-Rho1 was exchanged while bound to Glutathione-sepharose by incubating with either GTP, GDP, or GDP-pNPP in exchange buffer (50mM HEPES pH 7.08, 20mM $MgCl_2$ 5mM EDTA, 0.1mM EGTA, 50mM NaCl, 0.1mM DTT) for 30 minutes at 30ºC. Exchange was performed immediately prior to use in pulldown assays or prior to elution with glutathione.

Pyrene Actin Polymerization Assays. Rabbit skeletal muscle actin (5% pyrene labeled, Cytoskeleton) was resuspended in G-Buffer (2mM Tris pH 8.0, 0.1mM $CaCl_2$, 0.1mM ATP) at 4μM, and centrifuged at 120,000xg for 1 hour to remove endogenous nucleation centers. Actin/pyrene actin was incubated at room temperature in ME (1mM $MgCl_2$, 1mM EGTA) for 2 minutes to exchange bound calcium for magnesium. Polymerization was induced by addition of 10x KMEI (0.5M KCl, 10mM $MgCl_2$, 10mM EGTA, 100mM Imidazole, pH 7.0) at 1:10 of final volume. Test proteins (as above) were diluted into G-Buffer and added concomitantly with KMEI, keeping the final assay volumes constant throughout the experiment. Fluorescence was recorded with excitation at 365nm (minimum slit width, <2.5nm) and emission at 407nm (10nm slit width) using a Perkin Elmer LS-50B fluorescence spectrophotometer. Under these assay conditions the samples did not exhibit any photobleaching. Data were normalized taking the initial fluorescence level as zero and the half-maximal value of fluorescence for 100nM CapuFH2 to be 1.0 arbitrary units.

F-actin/Microtubule Co-sedimentation assays. Rabbit muscle actin (Cytoskeleton), at 22.5µM in G-Buffer, was polymerized by addition of 10xKMEI (as above) followed by 1 hour incubation at room temperature. Test proteins were diluted in G-Buffer and incubated with pre-assembled F-actin at 4µM for 30 minutes. Test proteins were centrifuged for 30' at 150,000xg prior to use in the assay to remove any aggregates. The F-actin/test protein mixture was centrifuged for 90 minutes at 150,000xg, and the supernatant and pellet fractions analyzed by SDS-PAGE. For low-speed co-sedimentation assays, the assay was performed as above except centrifuged at 20,000xg for 10 minutes. For microtubule co-sedimentation assays, bovine brain tubulin (Cytoskeleton) was suspended in PEM buffer (80mM PIPES, pH 7.0, 1mM EGTA, 1mM $MgCl_2$, 0.1mM GTP) at 18.2µM. Polymerization was induced by addition of tubulin polymerization inducer (80mM PIPES, pH 7.0, 1mM EGTA, 1mM $MgCl_2$, 0.1mM GTP + 50% glycerol) at 1:10 final volume, followed by 20 minute incubation at 35ºC. Microtubules were then diluted to 4µM and with G-PEM, stabilized with 2µM paclitaxel, and incubated with test proteins in G-PEM + 2µM paclitaxel for 30 minutes at room temperature. Test proteins were centrifuged for 30' at 100,000xg prior to use in the assay to remove any aggregates. The assay was then pipetted onto an equal volume of microtubule cushion buffer (G-PEM+10% glycerol + 2µM paclitaxel) and

centrifuged at 100,000xg for 45 minutes. The pellet and supernatant fractions were analyzed by SDS-PAGE or western blotting with anti GST antibody (1:1000-1:5000, ascites fluid, Babco).

F-actin/Microtubule crosslinking assays. F-actin and Microtubules were polymerized as above, except that Rhodamine-tubulin (Cytoskeleton) was mixed with unlabeled tubulin at 1:4. Microtubules were stabilized with taxol as above and F-actin stabilized with Alexa488-phalloidin. Microtubules (1 μM final concentration calculated by monomer), and test proteins (as indicated in the figure legend) were incubated in binding buffer (80mM PIPES pH 7.0, 1mM $MgCl_2$, 1mM EGTA, 2μM paclitaxel, 4U/100μL Alexa 488 phalloidin) for 15 minutes at room temperature, F-actin (1μM final concentration calculated by monomer) was then added, and incubated for an additional 10 minutes. The assays were then pipeted onto slides using a wide-orifice tip and visualized by fluorescence microscopy. For quantification, the cross-linking was carried out as above followed by low speed sedimentation (5,000 *g* for 10 minutes) as described[24]. The supernatant (S) and pellet (P) fractions were separated by SDS-PAGE followed by Coomassie blue staining.

GST-pulldown assays. GST-proteins bound to glutathione-sepharose were washed with HEPES-LS buffer (20mM HEPES pH 7.5, 150mM NaCl, 10% glycerol, 0.1% Triton X-100). Test proteins were synthesized *in vitro* using the TNT quick-coupled transcription-translation kit (Promega). For radiolabeling, ^{35}S-Methionine was included in the IVT reaction. IVT lysates post-translation were diluted in HEPES-LS + PMSF, Pepstatin, AEBSF, Leupeptin, and Aprotinin and pre-incubated with GST on glutathione sepharose for one hour at 4ºC to eliminate non-specific binding species. The pre-cleared lysates were then added to GST-protein in HEPES-LS and incubated at 4ºC for one hour. The sepharose matrix was then washed three times with HEPES-LS and the bound fraction analyzed by SDS-PAGE followed by autoradiography. In each case, 5% input (post-clearing with GST) is shown.

Immunoprecipitation. Ovary lysate was prepared by homogenizing dissected ovaries from ~200 females in 0.5mL L-buffer (PBS + 0.1% NP-40 + protease inhibitors (aprotinin, leupeptin, PMSF)), followed by sonication and centrifugation to pellet debris. Lysate was incubated with primary antibody in 0.5 mL L-buffer for 1hr at 4º C. Protein G sepharose was then added and the reaction allowed to proceed overnight at 4º C. Analysis was conducted using SDS-PAGE followed by Western blots.

ACKNOWLEDGEMENTS

We thank Juan Infante, Jeremy Nance, Suki Parks, Taryn Phippen, Jim Priess, Phil Soriano, and Valera Vasioukhin for their advice and interest during the course of this work and for comments on the manuscript. We also thank C. Berg, L. Cooley, A. Ephrussi, B. Kaiser, A. Koleske, P. Lasko, M. Maurer, L. Manseau, H. Oda, J. Roe, S. Roth, T. Schüpbach, L. Serbus, D. St. Johnston, R. Strong, W. Theurkauf, T. Tsukiyama, J. Vazquez, V. Vigdorovich, A. Wittinghofer, and the Bloomington Stock Center for advice, equipment, protocols, antibodies, DNAs, flies and other reagents used in this study. This work was supported by NIH grant GM066847 (to S.M.P).

REFERENCES

1. Theurkauf, W. E. Premature microtubule-dependent cytoplasmic streaming in cappuccino and spire mutant oocytes. *Science* **265,** 2093-2096 (1994).
2. Manseau, L. & Schüpbach, T. *cappuccino* and *spire*: two unique maternal-effect loci required for both the anteroposterior and dorsoventral patterns of the *Drosophila* embryo. *Genes Dev*. **3**, 1437-1452 (1989).
3. Emmons, S. *et al. cappuccino*, a *Drosophila* maternal effect gene required for polarity of the egg and embryo, is related to the vertebrate *limb deformity* locus. *Genes Dev.* **9,** 2482-2494 (1995).
4. Wellington, A. *et al*. Spire contains actin binding domains and is related to ascidian posterior end mark-5. *Development* **126,** 5267-74 (1999).
5. Cooley, L. & Theurkauf, W. E. Cytoskeletal functions during Drosophila oogenesis. *Science* **266**, 590-6 (1994).
6. Palacios, I. M. & St Johnston, D. *Kinesin light chain*-independent function of the *Kinesin heavy chain* in cytoplasmic streaming and posterior localisation in the *Drosophila* oocyte. *Development* **129**, 5473-5485 (2002).
7. Serbus, L., Cha, B., Theurkauf, W. & Saxton, W. Dynein and the actin cytoskeleton control kinesin-driven cytoplasmic streaming in Drosophila oocytes. *Development* **132**, 3743-52 (2005).
8. Manseau, L., Calley, J. & Phan, H. Profilin is required for posterior patterning of the *Drosophila* oocyte. *Development* **122**, 2109-2116 (1996).
9. Magie, C. R., Meyer, M. R., Gorsuch, M. S. & Parkhurst, S. M. Mutations in the Rho1 small GTPase disrupt morphogenesis and segmentation during early Drosophila development. *Development* **126**, 5353-5364 (1999).
10. Aktories, K., Wilde, C, & Vogelsgesang M. Rho-modifying C3-like ADP-ribosyl-transferases. *Rev. Physiol. Biochem. Pharmacol*. **152,** 1-22 (2004).
11. Quinlan, M., Heuser, J., Kerkhoff, E. & Mullins, R. Drosophila Spire is an actin nucleation factor. *Nature* **433**, 382-8 (2005).
12. Brand, A. H., Manoukian, A. S. & Perrimon, N. Ectopic expression in *Drosophila*. *Methods Cell Biol.* **44,** 635-54 (1994).
13. Wen, Y. et al. EB1 and APC bind to mDia to stabilize microtubules downstream of Rho and promote cell migration. *Nat Cell Biol*. **6**, 820-30 (2004).
14. Palazzo, A. F., Cook, T. A., Alberts, A. S. & Gundersen, G. G. mDia mediates Rho-regulated formation and orientation of stable microtubules. *Nat. Cell Biol.* **3,** 723-729 (2001).
15. Wittmann, T. & Waterman-Storer, C. M. Cell motility: can Rho GTPases and microtubules point the way? *J. Cell Sci.* **114,** 3795-3803 (2001).
16. Wallar, B. J. & Alberts, A. S. The formins: active scaffolds that remodel the cytoskeleton. *Trends Cell Biol.* **13,** 435-446 (2003).
17. Evangelista, M., Zigmond, S. & Boone, C. Formins: signaling effectors for assembly and polarization of actin filaments. *J. Cell Sci*. **116,** 2603-2611 (2003).

18. Zigmond, S. H. Formin-induced nucleation of actin filaments. *Curr. Opin. Cell Biol.* **16,** 99-105 (2004).

19. Magie, C. R., Pinto-Santini, D. & Parkhurst, S. M. Rho1 interacts with p120^{ctn} and α-catenin, and regulates cadherin-based adherens junction components in *Drosophila*. *Development* **129,** 3771-3782 (2002).

20. Li, F. & Higgs, H. N. The Mouse Formin mDia1 Is a Potent Actin Nucleation Factor Regulated by Autoinhibition. *Curr. Biol.* **13,** 1335-1340 (2003).

21. Ishizaki, T. *et al*. Coordination of microtubules and the actin cytoskeleton by the Rho effector mDia1. *Nat. Cell Biol.* **3,** 8-14 (2001).

22. Higgs, H. N. Formin proteins: a domain-based approach. *Trends Biochem. Sci.* **30,** 342-53 (2005).

23. Olson, M. F. GTPase Signalling: New Functions for Diaphanous-Related Formins. *Curr. Biol.* **13,** R360-R362 (2003).

24. Miller, A. L, Wang, Y., Mooseker, M. S. & Koleske, A. J. The Abl-related gene (Arg) requires its F-actin-microtubule cross-linking activity to regulate lamellipodial dynamics during fibroblast adhesion. *J. Cell Biol.* **165,** 407-419 (2004).

25. Schumacher, N., Borawski, J. M., Leberfinger, C. B., Gessler, M. & Kerkhoff, E. Overlapping expression pattern of the actin organizers Spir-1 and formin-2 in the developing mouse nervous system and the adult brain. *Gene Expr. Patterns* **4,** 249-55 (2004).

26. Leader, B. et al. Formin-2, polyploidy, hypofertility and positioning of the meiotic spindle in mouse oocytes. *Nat Cell Biol.* **4**, 921-8 (2002).

27. Ryley, D. et al. Characterization and mutation analysis of the human FORMIN-2 (FMN2) gene in women with unexplained infertility. *Fertil Steril.* **83**, 1363-71 (2005).

28. Spradling, A. C. P element-mediated transformation. In *Drosophila, a Practical Approach*, (ed. D. B. Roberts), pp. 175-197. Oxford: IRL Press (1986).

29. Grieder, N.C., de Cuevas, M. & Spradling, A. C. The fusome organizes the microtubule network during oocyte differentiation in *Drosophila*. *Development* **127,** 4253-4264 (2000).

30. Cha, B.-J., Serbus, L. R., Koppetsch, B. S. & Theurkauf, W. E. Kinesin I-dependent cortical exclusion restricts pole plasm to the oocyte posterior. *Nat. Cell Biol.* **4,** 592-598 (2002).

FIGURE LEGENDS

Figure 1 *Rho1-capu,* reduced *Rho1*, and *capu-spire* oocytes undergo premature ooplasmic streaming. (**a-e'**) Still confocal micrographs (**a-e**) and 5-frame confocal temporal projections of confocal time-lapse movies (**a'-e'**) of wildtype and mutant oocytes stained with trypan blue to visualize dynamic yolk granule movement. Granules appear as discrete spots of fluorescence in the still images. Linear patterns of light in the temporal projections indicate coordinated yolk granule movement generated by ooplasmic streaming. Anterior is up in all images. Wildtype stage 10 oocyte (**a**, **a'**) during cytoplasmic streaming. Note the spiral pattern formed by circular movement of yolk granules (**a'**). (**b-f'**) Unlike wildtype (**b**, **b'**), stage 7 oocytes from *Rho1-capu* (**c**, **c'**), reduced *Rho1* (**d**, **d'**), and *spir-capu* (**e**, **e'**) mutant mothers all undergo premature ooplasmic streaming, as indicated by the spiral patterns of fluorescence seen in the temporal projections (**c'**, **d'**, **e'**). (**f**) Schematic of a stage 10 egg chamber, consisting of the germline nurse cells (light gray) and oocyte (white), surrounded by somatic follicle cells (dark gray). Boxed area indicates region of egg chamber shown in panels **a-j**. Anterior is up. (**g-j**) Confocal micrographs of stage 7 oocytes from wildtype (**g**), *Rho1-capu* (**h**), reduced *Rho1* (**i**), and *spir-capu* (**j**) females stained with α-tubulin to visualize dynamic microtubules. Note subcortical arrays consistent with microtubule-dependent ooplasmic streaming (arrowheads in **h**-**j**). Scale bars: 50 μm.

Figure 2 Rho1, Capu and Spire expression is enriched at the oocyte cortex where stable microtubules are also localized. (**a-d'**) Rho1, Spire and Capu co-localize at the oocyte cortex. Stage 7 10 egg chambers from females containing transgenes expressing GFP-Capu (**a**), GFP-Spire isoform D (**b**), GFP-Spire isoform C (**c**), or GFP-Rho1 (**d**), and counterstained with phosphotyrosine (red; not used in **d, d'**) to outline the oocyte plasma membrane and DAPI (blue) to visualize the nuclei. Higher magnification views of the follicle cells and oocyte cortex are shown in **a'-d'**, respectively. We intermittently observe mosaicism of Rho1-GFP transgene expression in the somatic (follicle) cells (see Methods) as shown here to more clearly visualize Rho1 enrichment at the oocyte cortex. (**e-f**) Organization of the oocyte cortex. (**e**) High magnification view of the stage 10 wildtype oocyte cortex double labeled with α-tubulin (green) to visualize dynamic microtubules and Glu-tubulin (red) to visualize stabilized microtubules.

Note separation between apical follicle cell membrane (arrowhead) and cortical band of Glu-microtubules (arrow). (**f**) A schematic diagram of the oocyte cortex showing the relative locations of the cytoskeletal components. (**g**) Quantification of the relative pixel intensity for Glu-microtubule staining at the anterior cortex (boxed region "A") versus the posterior pole of the egg chambers (boxed region "P") such as those shown in **h-j.** Error bars represent the standard deviation from the mean obtained from quantifying 20 egg chambers. (**h-j'**) Confocal micrographs of stage 10 oocytes stained with antibodies recognizing detyrosinated (Glu-) tubulin to visualize stabilized microtubules. Stage 10 egg chambers from wildtype (**h**), reduced *Rho1* (**i**), and *Rho1-capu* (**j**) females. Anterior is to the left. (**h'-j'**) Higher magnification view of the oocyte cortex in **h-j**, respectively. (**h''-j''**) Close up view of the posterior pole of the oocytes in **h-j**, respectively. Note the reduced level of Glu-microtubules at the posterior in wildtype (**h''**) relative to the rest of the cortex. Levels of Glu-tubulin are not reduced at the posterior relative to the lateral cortex in *Rho1* or *Rho1-capu* (**i''-j''**, respectively). Scale bars: (**a-d**) 50 μm; (**a'-d'**) 20 μm; (**e**) 10 μm; (**h-j**) 20 μm; (**h'-j"**) 10 μm.

Figure 3 Protein-Protein interactions among Rho1, Capu, and Spire indicate a complex regulatory network. (**a**) Diagram of a canonical DRF protein and of the Capu protein. The Capu protein fragments used to map Capu/Spire/Rho1 protein-protein interactions are indicated. (**b**) Diagram of the Spire-A, -C, and -D protein isoforms. The Spire protein fragments used to map the Capu/Spire/Rho1 protein-protein interactions are indicated. (**c**) Rho1 binds directly to the N-terminus of Capu. ^{35}S labeled *in vitro* translated (IVT) CapuN3 (fourth panel from top) binds preferentially to GST-Rho^{GTP} (lane 4). This interaction is preserved in other Capu fragments that span CapuN3 (top 3 panels; lane 4). (**d**) All three Spire isoforms bind preferentially to Rho^{GTP}. ^{35}S labeled IVT-SpireA (top panel), SpireD (middle panel) and SpireC (bottom panel) bind to GST-Rho^{GTP} (lane 4). (**e-f**) Using the Spire protein pieces depicted in **b**, Rho1 binding to Spire-D and -C was mapped to the non-overlapping regions encompassed by SpireD3 (**e**) and SpireC3 (**f**). While we reproducibly observe low levels of Spire-D2 and -D4 binding to Rho1^{GTP}, neither of these proteins affects Capu's crosslinking or nucleation functions. (**g**) Immunoprecipitation from ovary lysate showing *in vivo* interaction between Rho1 and Capu. Capu is precipitated by an antibody to Rho1, but not when a non-relevant or no primary antibody is used. (**h**) Capu exhibits an intramolecular interaction. ^{35}S labeled IVT-CapuC2 (input; lane 1) binds to GST-

CapuN3 (lane 3). (**i**) The Capu FH2 domain binds directly to the WH2-containing SpireD3 domain. ^{35}S labeled IVT-CapuFH2 (input; lane 1) binds preferentially to GST-SpireD (lane 3) and GST-SpireD3 (lane 6). (**j**) Capu binding to Spire is disrupted by GTP-bound Rho1. ^{35}S labeled IVT-CapuFH2 (input; lane 1) binds to GST-SpireD (top panel, lane 3) and GST-SpireD3 (bottom panel, lane 3). The interaction between CapuFH2 and either SpireD or SpireD3 is disrupted by simultaneous addition of IVT-Rho1 in a dose-sensitive manner (lanes 4-6), and abolished when added after the interaction has stabilized (lane 7). (**k**) Capu FH2 domains dimerize. ^{35}S labeled IVT-CapuFH2 (input; lane 1) binds to GST-CapuFH2 (lane 3). This interaction is observed with wildtype, as well as mutant (L768H and P597T), FH2 domains.

Figure 4 Capu and Spire affect actin dynamics. **(a)** Pyrene-actin polymerization assays were conducted with varying concentrations of CapuFH2 (indicated in μM). **(b)** Capu actin nucleation activity is not subject to auto-inhibition. CapuFH2 (1 μM) was pre-incubated with CapuN1 (1 μM) in G-buffer, or an equal volume of G-buffer alone, and added to pyrene actin polymerization assays. CapuN1 alone (1 μM) had no affect on actin dynamics. **(c)** The *capu*^{2F} mutation does not affect actin nucleation. CapuFH2, CapuFH2[L768H], or CapuFH2[P597T], all at 1 μM, were added to polymerization assays. Note that the L768H mutation (corresponding to *capu*^{RK12}) abolished nucleation activity whereas the P597T mutation (corresponding to *capu*^{2F}) did not substantially affect nucleation. **(d)** CapuFH1-FH2 or was added to polymerization assays at varying concentrations (indicated in μM). **(e)** The affect of various concentrations of SpireD or SpireC (indicated in μM) on polymerization kinetics was assayed as above. **(f)** Capu and Spire do not affect each other's actin nucleation activity. CapuFH1-FH2 (0.1 μM) or SpireD (0.8 μM) alone, or CapuFH1-FH2 pre-incubated with SpireD, was added to pyrene actin polymerization assays.

Figure 5 Rho1 regulates crosslinking of F-actin and microtubules by Capu and Spire. (**a**-**n**) Microtubule and microfilament bundling and crosslinking properties of Capu, Spire and Rho1. Stabilized microtubules (1:5 rhodamine-labeled:unlabeled; 1 μM; middle column) and F-actin (1 μM; left column) were incubated with Capu, Spire and Rho1 proteins, the mixture was diluted 1:4, plated on glass coverslips then visualized by confocal microscopy. (**a**) No protein added; (**b**) CapuN1; (**c**) CapuFH2; (**d**) CapuN1 and CapuFH2; (**e**) CapuFH2^{2F} (CapuFH2 containing

P597T mutation); (**f**) CapuFH2^{RK12} (CapuFH2 containing L768H mutation); (**g**) SpireC isoform; (**h**) SpireD isoform; (**i**) CapuFH2 and SpireD; (**j**) CapuFH2 and Spire D1 protein piece; (**k**) CapuFH2 and Spire D3 protein piece; (**l**) CapuFH2 and Spire D with Rho1^{GTP}; (**m**) CapuFH2 and Spire D with Rho1^{GDP}; and (**n**) SpireC and SpireD. Final protein concentrations were: CapuFH2 (300 nM), CapuN (300 nM), CapuFH2-2F (300 nM), CapuFH2-LH (300 nM), SpireA (125 nM), SpireC (250 nM), SpireD (300 nM), SpireD1 (1 μM), SpireD3 (300 nM), and Rho1 (600 nM). Scale bar: 50 μm. Quantification of CapuFH2 wildtype and point mutant cross-linking by low speed co-sedimentation is shown in Supplementary Information Fig. S5b. (**o-p**) Model for the regulation of microtubule/microfilament crosslinking and ooplasmic streaming by Rho1, Capu, and Spire isoforms C and D. Schematic of a wildtype oocyte prior to the onset of ooplasmic streaming (**o**) and during ooplasmic streaming (**p**). Close-up views are shown in the insets. Microtubules are red and cortical microfilaments are green. Microtubule/microfilament crosslinking by SpireC and Capu is necessary to prevent the assembly of subcortical arrays of dynamic microtubules and the resulting streaming event (**o**). Active (GTP-bound) Rho1 promotes microtubule/microfilament crosslinking by sequestering SpireD, thereby preventing it from binding to SpireC and Capu. Upstream signaling events result in GTP hydrolysis by Rho1, allowing SpireD to bind to SpireC and Capu (**p**). This blocks microtubule/microfilament crosslinking, resulting in ooplasmic streaming.

Supplementary Information, Figure S1 *Rho1* and *Rho1-capu* mutants exhibit patterning defects similar to *capu*. (**a**) Schematic of a stage 10 egg chamber, consisting of the germline nurse cells (yellow) and oocyte (white), surrounded by somatic follicle cells (blue). Boxed area indicates regions shown in **b-g**. Anterior is up. (**b-g**) Confocal micrographs depicting posterior localization of Oskar (**b-d**) and Staufen (**e-g**) protein in stage 10 oocytes from wildtype (**b, e**), reduced *Rho1* (**c, f**), and *Rho1-capu* (**d, g**) females. Fc denotes follicle cells and ooc the oocyte in (**e**). (**h**) Schematic of a section at the posterior end of a cycle 14 embryo. Somatic epithelium is indicated in red and pole cells, the germline primordium, are indicated in green. (**i-k'**) Confocal photomicrograph projections (**i-k**) and cross-sections (**i'-k'**) of posterior end of cycle 14 embryos double labeled with antibodies to Vasa protein (green) to visualize pole cells and phosphotyrosine (red) to outline cells. Embryos derived from wildtype (**i, i'**), reduced *Rho1* (**j,**

j'), and *Rho1-capu* (**k, k'**) mothers. Embryos derived from reduced *Rho1* mothers have an average of 6 pole cells per embryo compared to 15 pole cells per embryo for wildtype and 0 pole cells per embryo for *Rho1-capu* (n=20 for each genotype). Scale bar: 50 μm.

Supplementary Information, Figure S2 Actin cytoskeleton is disrupted in *Rho1* and *Rho1-capu* egg chambers. (**a-f**) Confocal micrographs of stage 10 (**a-c**) and stage 7 (**d-f**) oocytes stained with phalloidin to visualize actin. FC indicates follicle cells and OOC denotes the oocyte (**a**). High-magnification view of the oocyte cortex of stage 10 egg chambers from wildtype (**a**), *Rho1* (**b**), and *Rho1-capu* (**c**) females. Note disorganization of the oocyte cortical actin in **b**, **c**. (**d-f**) Posterior end of stage 7 egg chambers from wildtype (**d**), *Rho1* (**e**), and *Rho1-capu* (**f**) females. Note the aberrant actin aggregation at the cortex in **e**, **f**. (**g-i'**) Microtubule organization is disrupted in *Rho1* and *Rho1-capu* egg chambers. Confocal micrographs of stage 10 oocytes stained with α-tubulin to visualize dynamic microtubules. Stage 10 egg chambers from wildtype (**g**), *Rho1* (**h**), and *Rho1-capu* (**i**) females. Anterior is to the left. Note accumulation and increased bundling of dynamic microtubules in the mutants. (**g'-i'**) Higher magnification view of the oocyte cortex in **g-i**, respectively. Note the high level of α-tubulin at the anterior cortex in wildtype (arrow in **g'**) that decreases in a gradient toward the posterior; the gradient is lost in the mutants. Scale bars: (**a-f**) 10 μm; (**g-i'**) 20 μm.

Supplementary Information, Figure S3 C3 transferase-injected oocytes undergo premature ooplasmic streaming. (**a-a'**) Still confocal micrographs (**a**) and 5-frame confocal temporal projections of confocal time-lapse movie (**a'**) of a C3 injected stage 7 oocyte undergoing premature ooplasmic streaming, as indicated by the spiral patterns of fluorescence seen in the temporal projection (**a'**). Anterior is up. (**b-e'**) Rho1, Capu and Spire expression is enriched at the oocyte cortex. Stage 7 egg chambers from females containing transgenes expressing GFP-Capu (**b**, **b'**), GFP-Spire isoform D (**c**, **c'**), GFP-Spire isoform C (**d**, **d'**), or GFP-Rho1 (**e**, **e'**), and counterstained with phosphotyrosine (red; not used in **d'-e'**) to outline the oocyte plasma membrane and DAPI (blue) to visualize the nuclei. Higher magnification views of the follicle cells and oocyte cortex are shown in **b'-e'**, respectively. Scale bars: (**a-a'**) 50 μm; (**b-e**) 50 μm; (**b'-e'**) 10 μm.

Supplementary Information, Figure S4 Protein-Protein interactions among Rho1, Capu, and Spire indicate a complex regulatory network. Non-cropped film images corresponding to the similarly marked GST-pulldown panels in Figure 3. As the gels shown range from 8-15% acrylamide, the molecular weights of the IVT proteins are indicated.

Supplementary Information, Figure S5 Rho1 regulates crosslinking of F-actin and microtubules by Capu and Spire. (**a**) Binding of CapuFH2 and CapuN, but not $Rho1^{GTP}$, to purified microfilaments in co-sedimentation assays. Western blot analysis of the total pellet of GST-CapuFH2, GST-CapuN or GST-$Rho1^{GTP}$ proteins incubated with F-actin followed by centrifugation (1:1000 anti-GST ascites; upper panel). Binding of CapuFH2, but not CapuN, to purified microtubules in co-sedimentation assays. Western blot analysis of the total pellet of GST-CapuFH2 and GST-CapuN proteins incubated with microtubules followed by centrifugation (1:1000 anti-GST ascites; lower panel). (**b**) Quantification of CapuFH2 wildtype and point mutant cross-linking by low speed co-sedimentation. CapuFH2 (wildtype), CapuFH2-2F and CapuFH2-LH were cross-linked as in Fig. 5 d, f, g, then the mixture was centrifuged to pellet microtubules and F-actin bundles cross-linked by the proteins as previously described[24]. The supernatant (S) and pellet (P) fractions were separated and the percent of CapuFH2 protein, microtubules, and F-actin found in the pellet fraction are given.

Supplementary Information, Figure S6 Model for the regulation of microtubule/microfilament crosslinking and ooplasmic streaming by Rho1, Capu, and Spire isoforms C and D. In this model, microtubule/microfilament crosslinking by SpireC and Capu is necessary to prevent the assembly of subcortical arrays of dynamic microtubules and the resulting streaming event. (**a**-**e**) Diagrams of the oocyte cortex in the various mutants used in this study. Relevant proteins are diagrammed and labeled (**f**). In each case, genetic mutation reduces crosslinking activity and allows the premature assembly of subcortical microtubule arrays and concomitant onset of ooplasmic streaming. (**a**) Reduced Rho1 levels liberate the majority of SpireD. SpireD binds to SpireC and Capu, blocking microtubule/microfilament crosslinking. (**b**) In oocytes lacking Capu, microtubule/microfilament crosslinking is reduced directly by removal of a protein with crosslinking activity. (**c**) Reducing both Rho1 and Capu by half results in decreased crosslinking both by decreasing the level of Capu and liberating more

SpireD to inhibit crosslinking by Capu and SpireC. (**d**) Removal of Spire (both C and D isoforms) results directly in reduced crosslinking by removing SpireC. The absence of SpireD prior to stage 10b is unlikely to have a substantial impact on the crosslinking activity of Capu because GTP-bound Rho1 sequesters SpireD during these stages. (**e**) Reducing Capu and Spire (both isoforms) by half directly causes reduced crosslinking. As described in **d** above, the reduction in SpireD is likely to have little effect in this instance during stages 7-10b.

Supplementary Information, Movie 1a Normal ooplasmic streaming in a wildtype stage 10 oocyte corresponding to the panels shown in Fig. 1a-a'. Note the spiral pattern formed by circular movement of yolk granule stained with trypan blue. This 22 second time-lapse movie represents 30 minutes of real time.

Supplementary Information, Movie 1b Wildtype stage 7 oocyte corresponding to the panels shown in Fig. 1b-b'. Note the yolk granules stained with trypan blue do not exhibit coordinated movements at this stage. This 14 second time-lapse movie represents 15 minutes of real time.

Supplementary Information, Movie 1c Premature ooplasmic streaming in a stage 7 *Rho1-capu* oocyte corresponding to the panels shown in Fig. 1c-c'. Note the spiral pattern formed by circular movement of yolk granule stained with trypan blue. This 22 second time-lapse movie represents 30 minutes of real time.

Supplementary Information, Movie 1d Premature ooplasmic streaming in a stage 7 *reduced Rho1* oocyte corresponding to the panels shown in Fig. 1d-d'. Note the spiral pattern formed by circular movement of yolk granule stained with trypan blue. This 22 second time-lapse movie represents 30 minutes of real time.

Supplementary Information, Movie 1e Premature ooplasmic streaming in a stage 7 *spir-capu* oocyte corresponding to the panels shown in Fig. 1e-e'. Note the spiral pattern formed by circular movement of yolk granule stained with trypan blue. This 29 second time-lapse movie represents 30 minutes of real time.

Supplementary Information, Movie 1f Premature ooplasmic streaming in a stage 7 wildtype oocyte injected with C3 transferase (a specific peptide inhibitor of Rho) corresponding to the panels shown in Supplementary Information, Fig. 3a-a'. Note the spiral pattern formed by circular movement of yolk granule stained with trypan blue. This 29 second time-lapse movie represents 30 minutes of real time.

Figure 1
(Rosales-Nieves et al.)

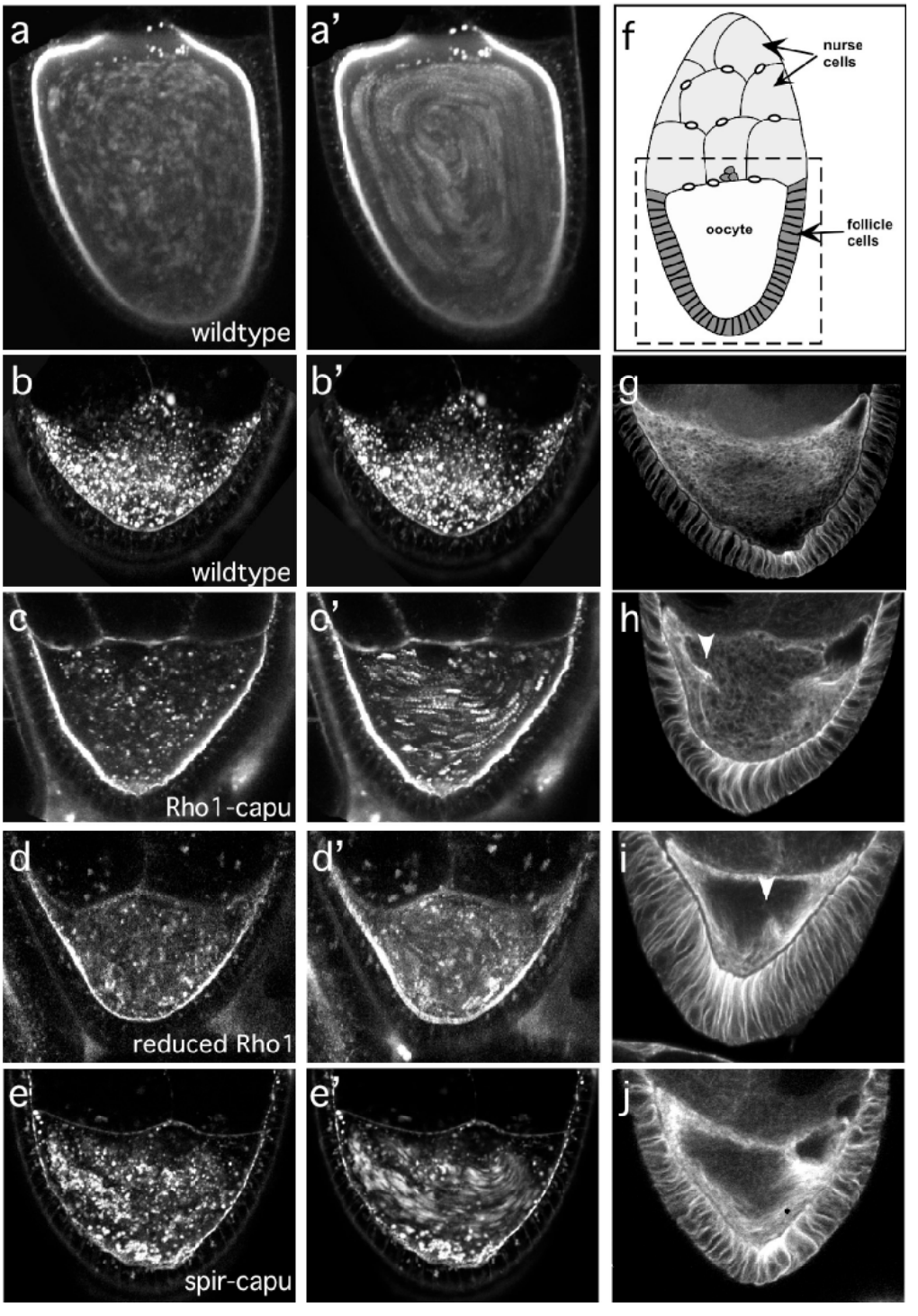

Figure 2
(Rosales-Nieves et al.)

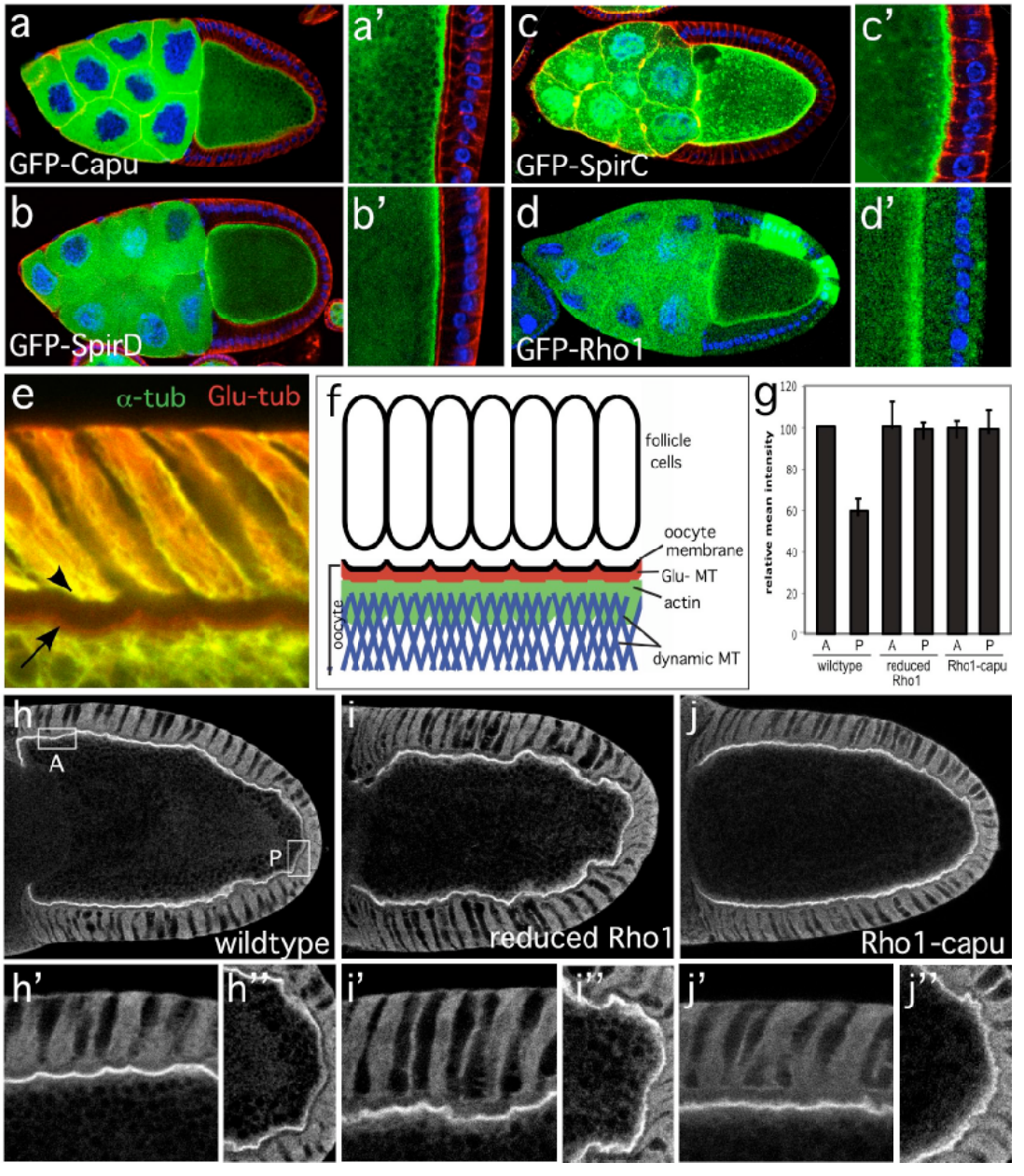

Figure 3
(Rosales-Nieves et al.)

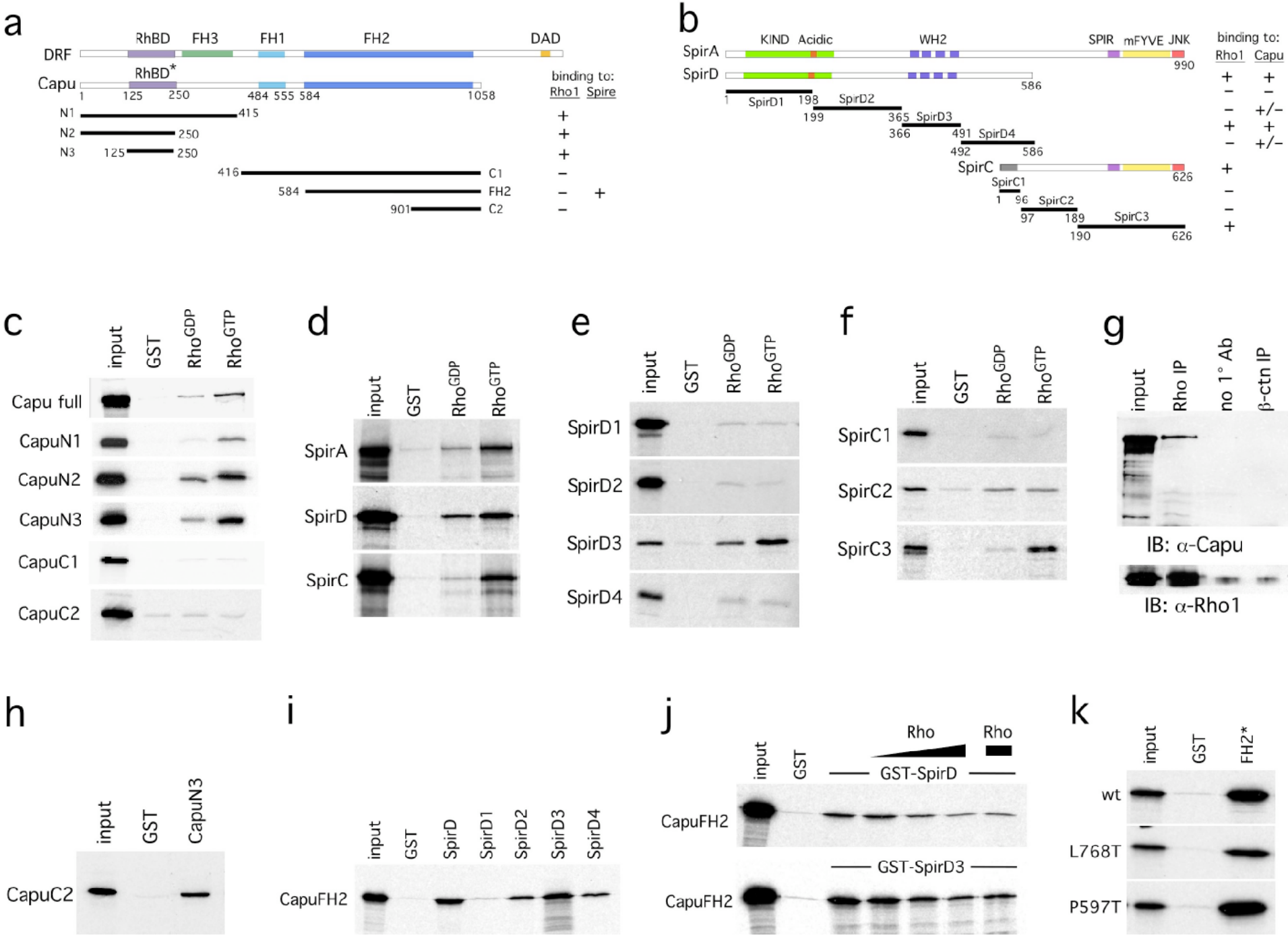

Figure 4
(Rosales-Nieves et al.)

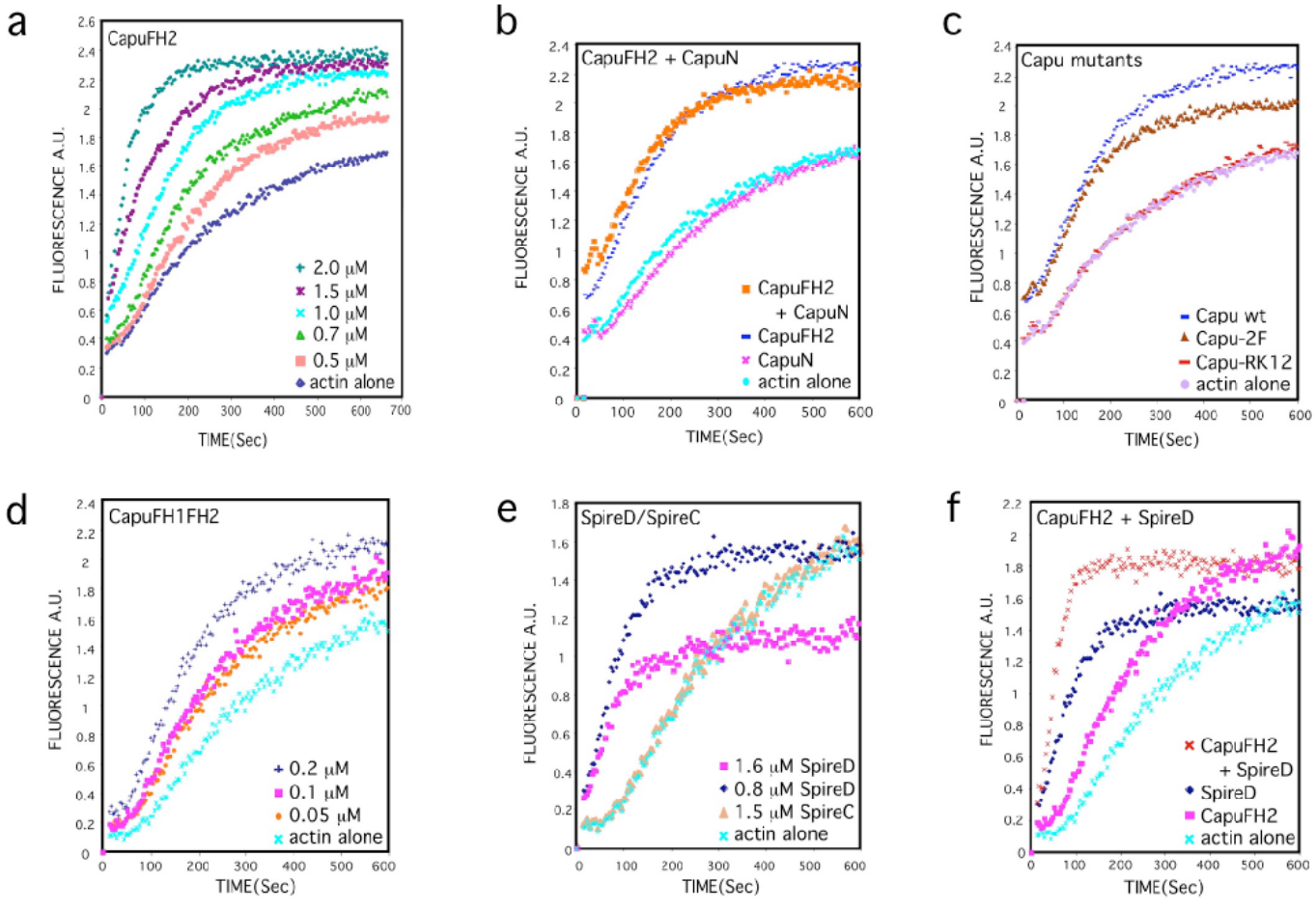

Figure 5
(Rosales-Nieves et al.)

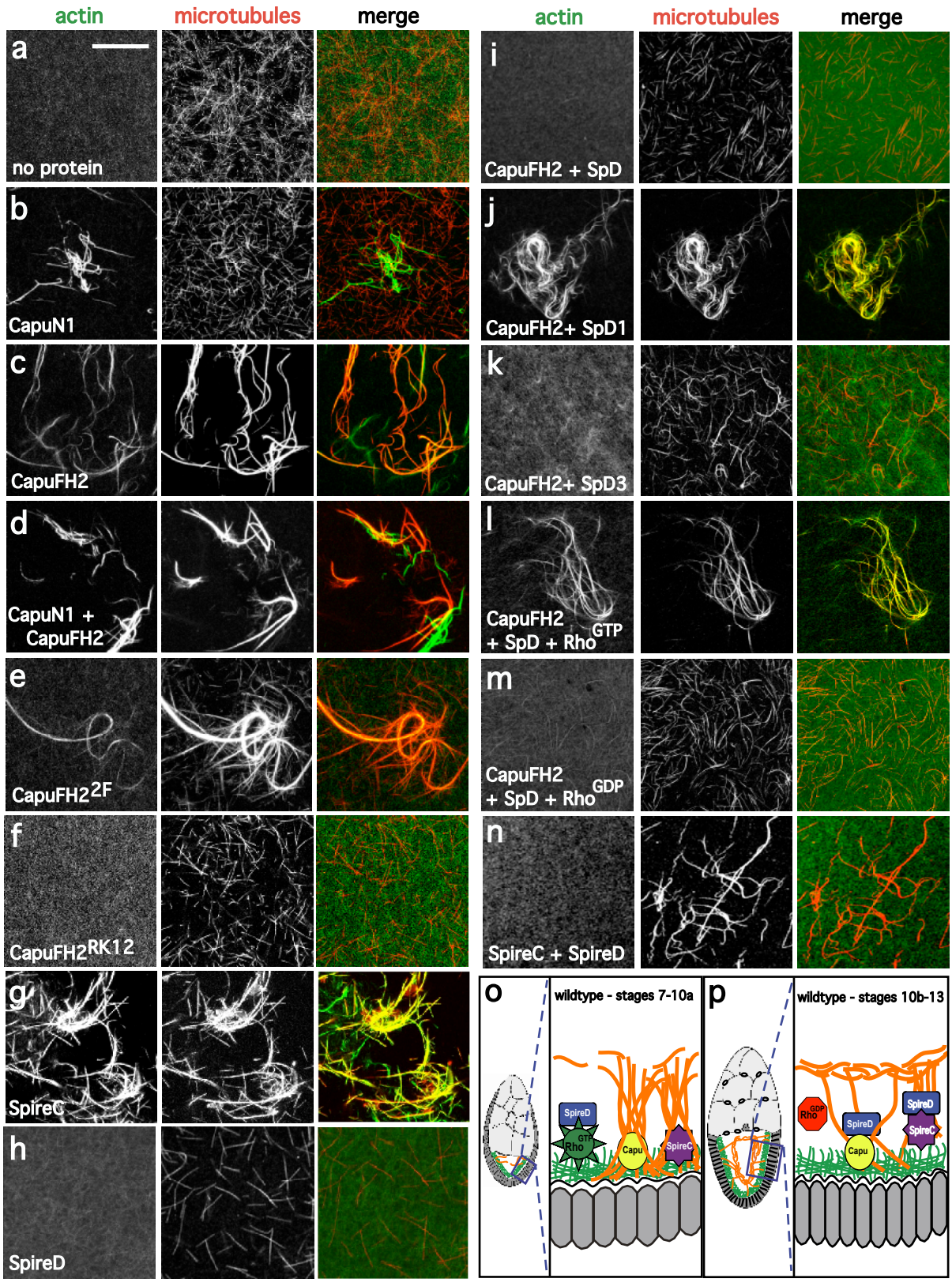

Supplementary Information

(Rosales-Nieves et al.)

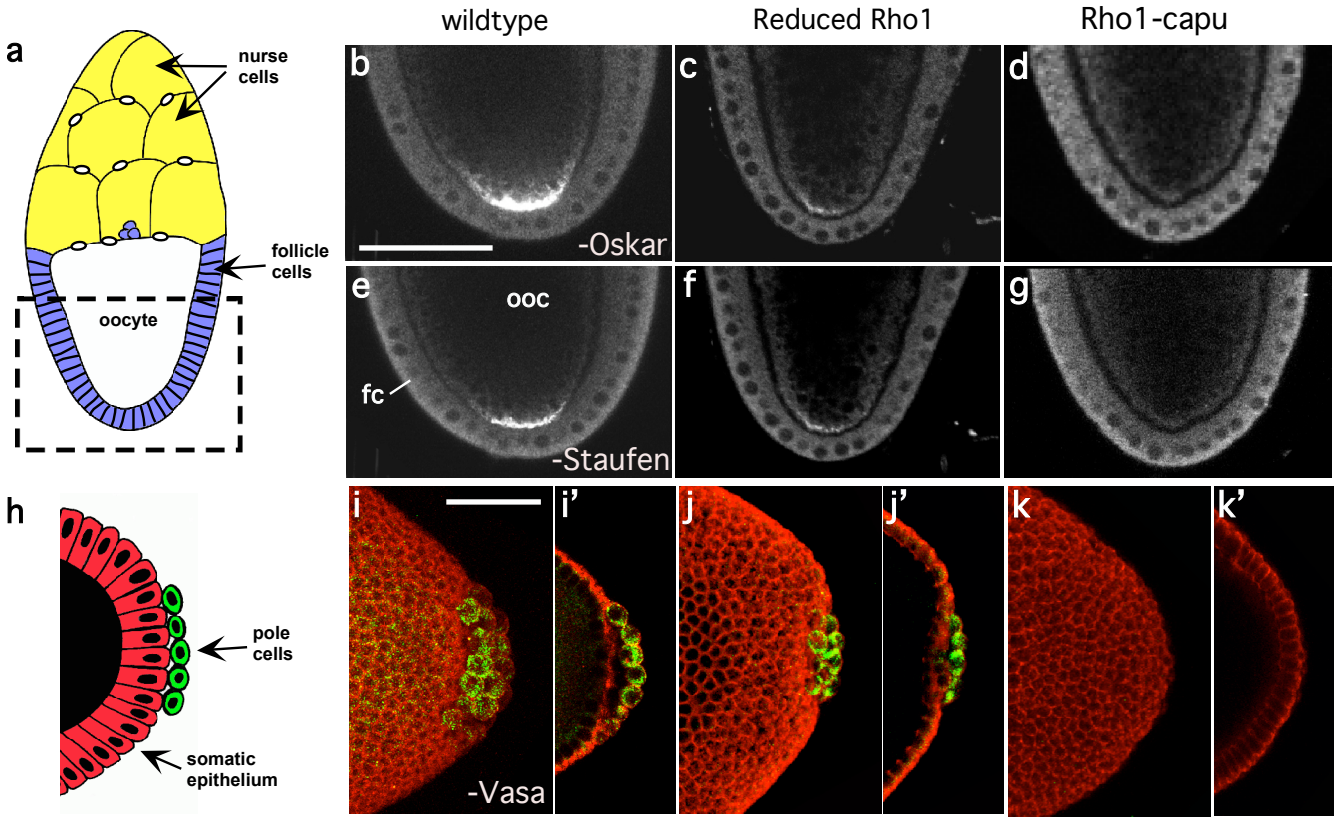

Supplementary Information, Figure S1 *Rho1* and *Rho1-capu* mutants exhibit patterning defects similar to *capu*. (**a**) Schematic of a stage 10 egg chamber, consisting of the germline nurse cells (yellow) and oocyte (white), surrounded by somatic follicle cells (blue). Boxed area indicates regions shown in **b-g**. Anterior is up. (**b-g**) Confocal micrographs depicting posterior localization of Oskar (**b-d**) and Staufen (**e-g**) protein in stage 10 oocytes from wildtype (**b, e**), reduced *Rho1* (**c, f**), and *Rho1-capu* (**d, g**) females. Fc denotes follicle cells and ooc the oocyte in (**e**). (**h**) Schematic of a section at the posterior end of a cycle 14 embryo. Somatic epithelium are indicated in red and pole cells, the germline primodium, are indicated in green. (**i-k'**) Confocal photomicrograph projections (**i-k**) and cross-sections (**i'-k'**) of posterior end of cycle 14 embryos double labeled with antibodies to Vasa protein (green) to visualize pole cells and phosphotyrosine (red) to outline cells. Embryos derived from wildtype (**i, i'**), reduced *Rho1* (**j, j'**), and *Rho1-capu* (**k, k'**) mothers. Embryos derived from reduced *Rho1* mothers have an average of 6 pole cells per embryo compared to 15 pole cells per embryo for wildtype and 0 pole cells per embryo for *Rho1-capu* (n=20 for each genotype). Scale bar: 50 m.

Supplementary Information

(Rosales-Nieves et al.)

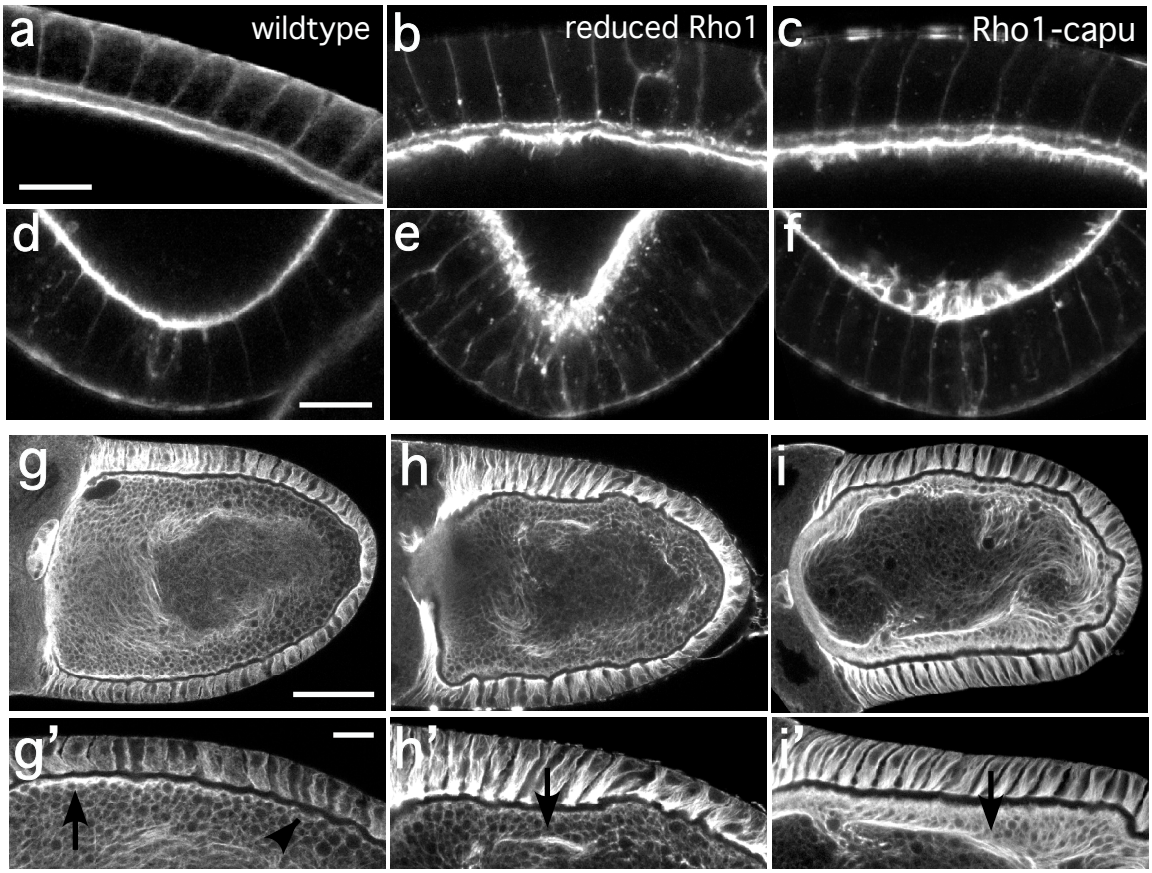

Supplementary Information, Figure S2 Actin cytoskeleton is disrupted in *Rho1* and *Rho1-capu* egg chambers. (**a-f**) Confocal micrographs of stage 10 (**a-c**) and stage 7 (**d-f**) oocytes stained with phalloidin to visualize actin. FC indicates follicle cells and OOC denotes the oocyte (**a**). High-magnification view of the oocyte cortex of stage 10 egg chambers from wildtype (**a**), *Rho1* (**b**), and *Rho1-capu* (**c**) females. Note disorganization of the oocyte cortical actin in **b**, **c**. (**d-f**) Posterior end of stage 7 egg chambers from wildtype (**d**), *Rho1* (**e**), and *Rho1-capu* (**f**) females. Note the aberrant actin aggregation at the cortex in **e**, **f**. (**g-i'**) Microtubule organization is disrupted in *Rho1* and *Rho1-capu* egg chambers. Confocal micrographs of stage 10 oocytes stained with -tubulin to visualize dynamic microtubules. Stage 10 egg chambers from wildtype (**g**), *Rho1* (**h**), and *Rho1-capu* (**i**) females. Anterior is to the left. Note accumulation and increased bundling of dynamic microtubules in the mutants. (**g'-i'**) Higher magnification view of the oocyte cortex in **g-i**, respectively. Note the high level of -tubulin at the anterior cortex in wildtype (arrow in **g'**) that decreases in a gradient toward the posterior; the gradient is lost in the mutants. Scale bars: (**a-f**) 10 m; (**g-i'**) 20 m.

Supplementary Information

(Rosales-Nieves et al.)

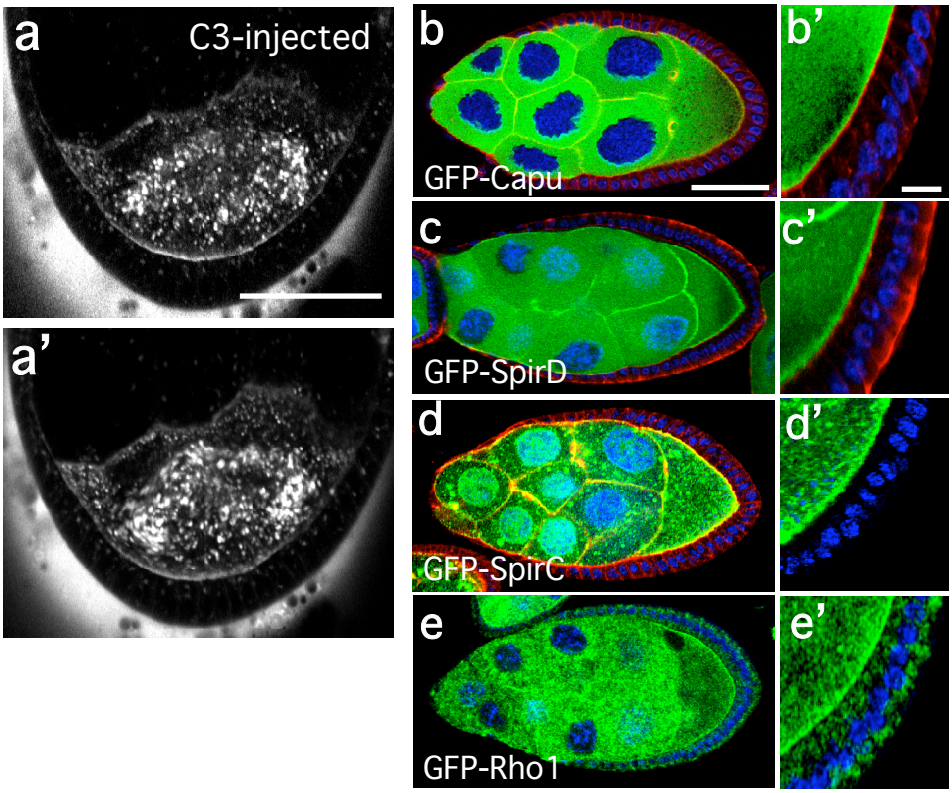

Supplementary Information, Figure S3 C3 transferase-injected oocytes undergo premature ooplasmic streaming. (**a-a'**) Still confocal micrographs (**a**) and 5-frame confocal temporal projections of confocal time-lapse movie (**a'**) of a C3 injected stage 7 oocyte undergoing premature ooplasmic streaming, as indicated by the spiral patterns of fluorescence seen in the temporal projection (**a'**). Anterior is up. (**b-e'**) Rho1, Capu and Spire expression is enriched at the oocyte cortex. Stage 7 egg chambers from females containing transgenes expressing GFP-Capu (**b**, **b'**), GFP-Spire isoform D (**c**, **c'**), GFP-Spire isoform C (**d**, **d'**), or GFP-Rho1 (**e**, **e'**), and counterstained with phosphotyrosine (red; not used in **d'-e'**) to outline the oocyte plasma membrane and DAPI (blue) to visualize the nuclei. Higher magnification views of the follicle cells and oocyte cortex are shown in **b'-e'**, respectively. Scale bars: (**a-a'**) 50 m; (**b-e**) 50 m; (**b'-e'**) 10 m.

Supplementary Information

(Rosales-Nieves et al.)

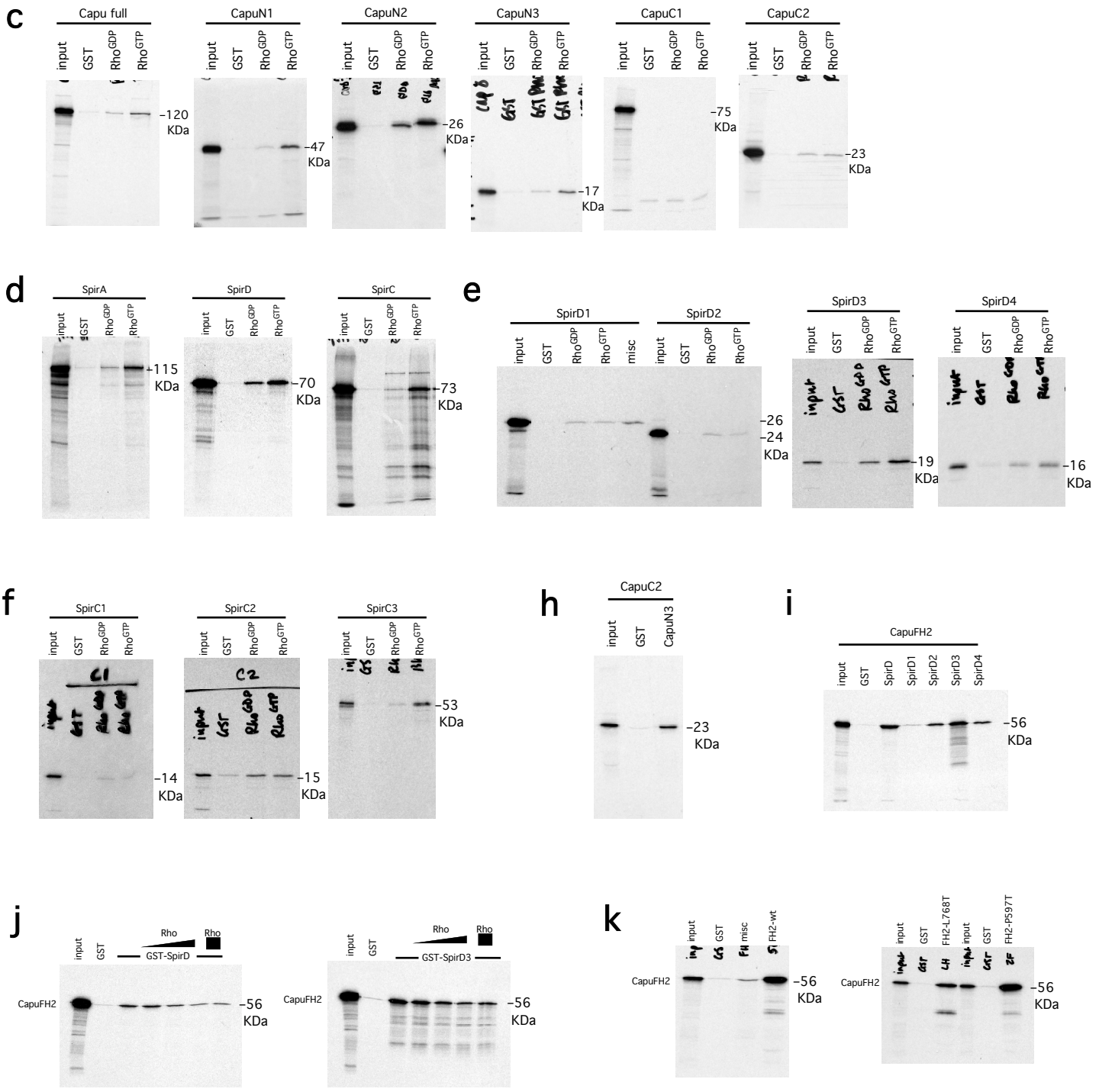

Supplementary Information, Figure S4 Protein-Protein interactions among Rho1, Capu, and Spire indicate a complex regulatory network. Non-cropped film images corresponding to the similarly marked GST-pulldown panels in Figure 3. As the gels shown range from 8-15% acrylamide, the molecular weights of the IVT proteins are indicated.

Supplementary Information

(Rosales-Nieves et al.)

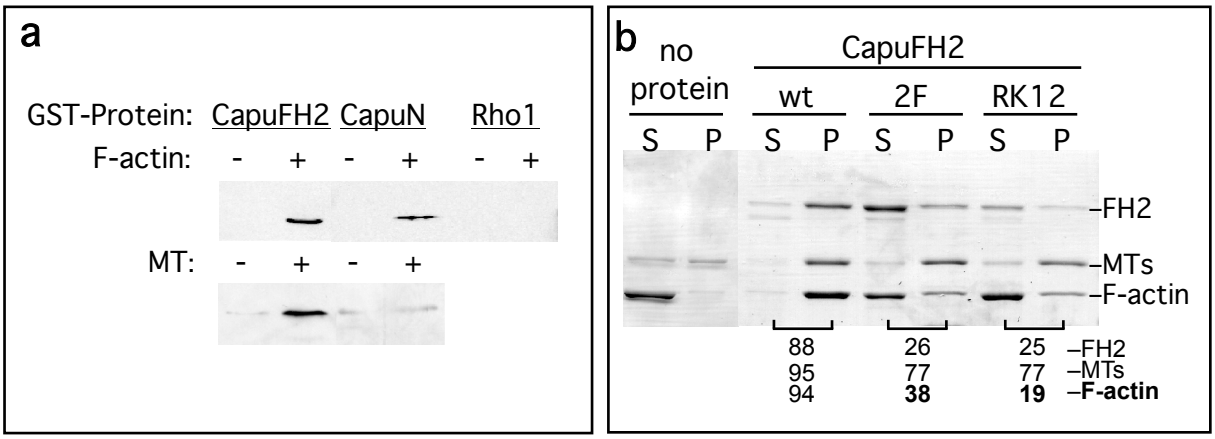

Supplementary Information, Figure S5 Rho1 regulates crosslinking of F-actin and microtubules by Capu and Spire. (**a**) Binding of CapuFH2 and CapuN, but not Rho1GTP, to purified microfilaments in co-sedimentation assays. Western blot analysis of the total pellet of GST-CapuFH2, GST-CapuN or GST-Rho1GTP proteins incubated with F-actin followed by centrifugation (1:1000 anti-GST ascites; upper panel). Binding of CapuFH2, but not CapuN, to purified microtubules in co-sedimentation assays. Western blot analysis of the total pellet of GST-CapuFH2 and GST-CapuN proteins incubated with microtubules followed by centrifugation (1:1000 anti-GST ascites; lower panel). (**b**) Quantification of CapuFH2 wildtype and point mutant cross-linking by low speed co-sedimentation. CapuFH2 (wildtype), CapuFH2-2F and CapuFH2-LH were cross-linked as in Fig. 5 d, f, g, then the mixture was centrifuged to pellet microtubules and F-actin bundles cross-linked by the proteins as previously described . The supernatant (S) and pellet (P) fractions were separated and the percent of CapuFH2 protein, microtubules, and F-actin found in the pellet fraction are given.

Supplementary Information

(Rosales-Nieves et al.)

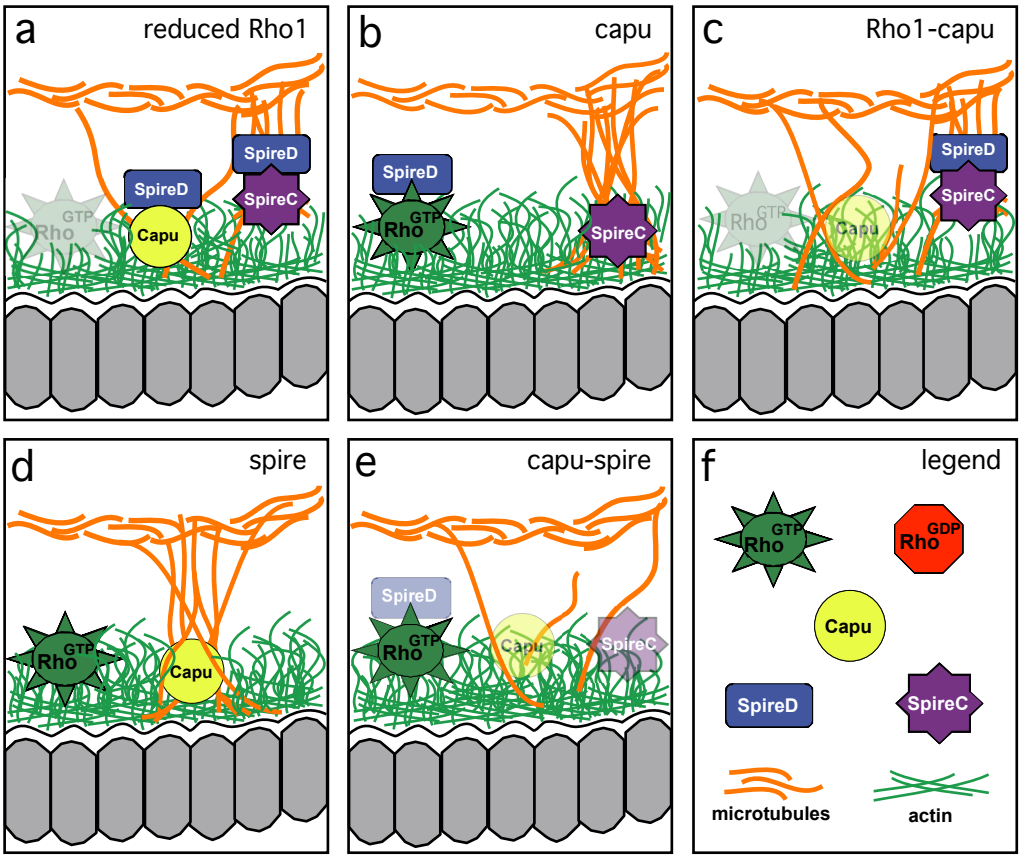

Supplementary Information, Figure S6 Model for the regulation of microtubule/microfilament crosslinking and ooplasmic streaming by Rho1, Capu, and Spire isoforms C and D. In this model, microtubule/microfilament crosslinking by SpireC and Capu is necessary to prevent the assembly of subcortical arrays of dynamic microtubules and the resulting streaming event. (**a**-**e**) Diagrams of the oocyte cortex in the various mutants used in this study. Relevant proteins are diagrammed and labeled (**f**). In each case, genetic mutation reduces crosslinking activity and allows the premature assembly of subcortical microtubule arrays and concomitant onset of ooplasmic streaming. (**a**) Reduced Rho1 levels liberate the majority of SpireD. SpireD binds to SpireC and Capu, blocking microtubule/microfilament crosslinking. (**b**) In oocytes lacking Capu, microtubule/microfilament crosslinking is reduced directly by removal of a protein with crosslinking activity. (**c**) Reducing both Rho1 and Capu by half results in decreased crosslinking both by decreasing the level of Capu and liberating more SpireD to inhibit crosslinking by Capu and SpireC. (**d**) Removal of Spire (both C and D isoforms) results directly in reduced crosslinking by removing SpireC. The absence of SpireD prior to stage 10b is unlikely to have a substantial impact on the crosslinking activity of Capu because GTP-bound Rho1 sequesters SpireD during these stages. (**e**) Reducing Capu and Spire (both isoforms) by half directly causes reduced crosslinking. As described in **d** above, the reduction in SpireD is likely to have little effect in this instance during stages 7-10b.